Journal of General Virology (2004), 85, 3049–3058 DOI 10.1099/vir.0.80169-0

Single point mutation in tick-borne encephalitis virus prM protein induces a reduction of virus particle secretion

Kentarou Yoshii,[1] Akihiro Konno,[2] Akiko Goto,[1] Junko Nio,[2] Mayumi Obara,[1] Tomotaka Ueki,[1] Daisuke Hayasaka,[3] Tetsuya Mizutani,[1] Hiroaki Kariwa[1] and Ikuo Takashima[1]

Correspondence
Ikuo Takashima
takasima@vetmed.hokudai.ac.jp

[1,2]Laboratory of Public Health, Department of Environmental Veterinary Sciences[1] and Laboratory of Anatomy[2], Graduate School of Veterinary Medicine, Hokkaido University, Sapporo 060-0818, Japan

[3]Department of Pathology, Institute of Tropical Medicine, Nagasaki University, 1-12-4 Sakamoto, Nagasaki 852-8523, Japan

Flaviviruses are assembled to bud into the lumen of the endoplasmic reticulum (ER) and are secreted through the vesicle transport pathway. Virus envelope proteins play important roles in this process. In this study, the effect of mutations in the envelope proteins of tick-borne encephalitis (TBE) virus on secretion of virus-like particles (VLPs), using a recombinant plasmid expression system was analysed. It was found that a single point mutation at position 63 in prM induces a reduction in secretion of VLPs. The mutation in prM did not affect the folding of the envelope proteins, and chaperone-like activity of prM was maintained. As observed by immunofluorescence microscopy, viral envelope proteins with the mutation in prM were scarce in the Golgi complex, and accumulated in the ER. Electron microscopic analysis of cells expressing the mutated prM revealed that many tubular structures were present in the lumen. The insertion of the prM mutation at aa 63 into the viral genome reduced the production of infectious virus particles. This data suggest that prM plays a crucial role in the virus budding process.

Received 6 April 2004
Accepted 28 June 2004

INTRODUCTION

Enveloped viruses acquire their lipid envelopes by budding through the plasma membrane or the membrane of an intracellular organelle, such as the endoplasmic reticulum (ER), the ER to Golgi intermediate compartment or the Golgi complex (Garoff *et al.*, 1998). Flaviviruses are generally thought to bud into the ER of infected cells (Lindenbach & Rice, 2001). Virus particles have been detected by electron microscopy in the lumen of the rough ER, and in the lumen of either the smooth ER or the intermediate compartment (Ishak *et al.*, 1988; Wang *et al.*, 1997). However, the details of the mechanism of the budding process are still almost unknown.

It has been reported that the envelope proteins play an important role in the budding process of many viruses. Expression of the M and E envelope proteins of mouse hepatitis virus, without other viral proteins, led to the secretion of virus-like particles (VLPs), which were morphologically similar to native virions (de Haan *et al.*, 1998; Vennema *et al.*, 1996). The hepatitis B virus (HBV) surface proteins can be secreted as subviral particles, but their morphology is quite different from HBV virions (Patzer *et al.*, 1986; Simon *et al.*, 1988). In the case of flaviviruses, slowly sedimenting haemagglutinin (sHA), which lacks infectivity, is secreted from virus-infected cells (Gritsun *et al.*, 1989; Heinz & Kunz, 1977). sHA has viral envelope proteins but lacks nucleocapsid protein and viral RNA, and its particulate structure is similar to the infectious virion, except for lower density and smaller size. Expression of the prM and E protein of several flaviviruses without other viral proteins results in the secretion of VLPs, which are similar to sHA particles (Allison *et al.*, 1995b; Konishi *et al.*, 1992; Mason *et al.*, 1991).

The flavivirus envelope has two proteins: the major envelope glycoprotein E (molecular mass 52 kDa) and the small membrane protein M (molecular mass 7–8 kDa). Both proteins are synthesized as part of a polyprotein precursor and then co- and post-translationally cleaved into the individual proteins (Lindenbach & Rice, 2001). The M protein is cleaved first into an intermediate precursor called prM, before final processing.

E protein is a well-characterized viral protein in flavivirus. E protein mediates virus entry via receptor-mediated endocytosis and also carries the major antigenic epitopes leading to a protective immune response (Heinz & Mandl, 1993).

The X-ray crystallographic resolution of the structure of the E ectodomain of TBE virus revealed that E protein forms head-to-tail homodimers that lie parallel to the viral envelope (Rey *et al.*, 1995). In low-pH condition, such as in endocytic vesicles, these homodimers dissociate and lead to the irreversible formation of homotrimers (Allison *et al.*, 1995a; Stiasny *et al.*, 2001, 2002).

M is synthesized as precursor protein, prM (molecular mass 25 kDa) in ER, carrying one *N*-linked oligosaccharide. One of the roles of prM protein reported previously is a chaperone-like activity for the folding and maturation of E (Konishi & Mason, 1993; Lorenz *et al.*, 2002). Newly synthesized E and prM proteins associate to form heterodimers that are incorporated into immature virions (Wengler & Wengler, 1989). This heterodimerization leads to the final native conformation of E and protects E from inactivation by acidification in the transport vesicles (Heinz & Allison, 2000). Shortly before release from the cell, the immature particles are converted to the active form by cleavage of the pr-portion from prM by a cellular furin protease in *trans*-Golgi network and prM turns into M (Elshuber *et al.*, 2003; Stadler *et al.*, 1997).

Recent examination of the assembly and maturation of Kunjin virus revealed that the assembly of virions occurs within the lumen of the rough ER (Mackenzie & Westaway, 2001). Furthermore, the structure of immature flavivirus particles containing prM was analysed by cryoelectron microscopy (Zhang *et al.*, 2003). Sixty trimeric spikes were organized icosahedrally on the surface of the particles, in contrast to the smooth surface of mature virions reported previously (Kuhn *et al.*, 2002). In the spike structure, prM covers the fusion peptides of E in a manner similar to the organization of the glycoproteins in alphavirus spikes (Zhang *et al.*, 2002). In this way, various approaches have revealed the morphological assembly and maturation processes of virus particles, but the molecular mechanism of virus budding and secretion remains obscure.

In this study, we constructed plasmids expressing mutant prM and E proteins of TBE virus, and tested the effect of these mutations on the production of VLPs when expressed in mammalian cells. This allowed the identification of a single point mutation in prM that induced a reduction of secretion of VLPs. The mutation in prM did not affect the oxidative folding of the viral envelope proteins nor the chaperone-like activity of prM. The envelope proteins not secreted from the cells due to the prM mutation accumulated in the ER, and the transport of viral envelope proteins to the Golgi complex was also inhibited. By electron microscopy, tubular structures were observed in the lumen of the ER. When the point mutation in prM was introduced into the TBE virus genome, it severely reduced the ability of the mutant viral RNA to produce infectious particles. This data points out the critical role of prM protein in the virus budding process.

METHODS

Cells. Baby hamster kidney (BHK)-21 cells were grown at 37 °C in MEM supplemented with 8% FCS and 2 mM L-glutamine. 293T cells were cultured at 37 °C in Dulbecco's Modified Eagle's Medium, containing 10% FCS, 2 mM L-glutamine and penicillin–streptomycin (50 U and 50 μg ml^{-1}, respectively).

Antibodies. For detection of TBE virus prM and E proteins, ELISA, immunoprecipitation and immunofluorescence experiments, mouse anti-E mAb 1H4 and 4H8, prepared in our laboratory, were used (Komoro *et al.*, 2000). Rabbit polyclonal anti-prM and anti-E antibodies were prepared by immunization with recombinant prM and E proteins expressed in the pET43 system (Novagen). For the immunofluorescence colocalization studies, anti-calreticulin rabbit polyclonal antiserum (Affinity BioReagents) or anti-giantin rabbit polyclonal antiserum (Covance Research Products) was applied. FITC conjugated anti-mouse IgG antibodies and Texas red conjugated anti-rabbit IgG antibodies (Jackson Immunoresearch) were used as secondary antibodies in the immunofluorescence assays.

Plasmid construction. The production of the recombinant plasmid pCAGprME expressing prM and full-length E, derived from the Oshima 5-10 strain of TBE virus (GenBank accession no. AB062063), was described previously (Yoshii *et al.*, 2003). For the construction of the mutant plasmids, TBE viral RNA was extracted from virus-inoculated suckling mouse brain and RT-PCR was performed as described previously (Takashima *et al.*, 1997). Amplification of mutated DNA coding prM and E gene was carried out twice by error-prone PCR using *Xho*IMEf and *Cla*IrNS1 primers (Table 1), with AmpliTaq DNA polymerase (Applied Biosystems), in the presence of a high concentration of Mg^{2+}, at low annealing temperature. To generate the mutant expression plasmid, clone 55, the PCR products were then digested with *Xho*I and *Cla*I, and cloned into the pCAGGS/MCSR plasmid (Niwa *et al.*, 1991).

For the construction of pCAGprMEpr63S, DNA fragments with the site-directed mutation were amplified by PCR using pr63Sf and pr63Sr primers (Table 1). The PCR products were digested by *Xho*I and *Psh*AI and inserted into the pCAGprME wild-type plasmid, also treated with *Xho*I and *Psh*AI. For the pr88E and E276V464P plasmids, DNA fragments amplified using appropriate primers (M160f and M4 for pr88S; 5s and *Cla*IrNS1 for E276V464P, Table 1) were digested by

Table 1. Primers used in this study

Primer	Primer sequence* (5′–3′)
*Xho*IMEf	agcctcgag*atg*GTAGGTTTGCAAAGACG (*Xho*I)
*Cla*IrNS1	ctcatcgat*cta*ATAATTGTCATACCACTCGGATA-CCTCCC (*Cla*I)
pr63Sf†	TAGACCAGGGGGAGGAAtCGGTT
pr63Sr†	CG*a*TTCCTCCCCCTGGTCTA
M160f	AGGGGGAGGAACCGGTTGAC (*Age*I)
M-4	CATTGAGGGCTTCCCCTCAG
5s	CGGAGACCTGTCCTTGTTAT

*Viral and nonviral sequences are in upper case and lower case, respectively. Restriction endonuclease sites are underlined and indicated in parentheses. Italics show the start and stop codons.
†Mutations within the viral sequences are depicted in italicized lower case.

restriction enzymes (*Age*I and *Psh*AI for pr88E; *Bst*Z17I for E276V464P) and inserted into the pCAGprME wild-type plasmid, as described above.

For the construction of the TBE virus infectious cDNA clone containing the Pro→Ser mutation at position 63 in prM, the site-directed mutation was substituted into pGEMT-CprME using the pr63Sf and pr63Sr primers described above. The reconstructed plasmid was then digested with *Spe*I and the fragment containing the mutation was replaced into Oshima IC-pt, as described previously (Hayasaka *et al.*, 2004). The new cDNA clone construct was designated Oshima IC-pr63S.

Transfection. 293T cells, grown to 60–70 % confluence in six-well culture plates, were transfected with 2 μg each plasmid complexed to *Trans*IT-LT1 reagent (PanVera) in Opti-MEM (Invitrogen). At 24 h post-transfection (or as otherwise stated), the cells and supernatant were harvested and used for further experiments.

ELISA. Transfected cells were lysed with 1 % Triton X-100 in 10 mM Tris-buffered saline (TBS) and the supernatants were treated with 1 % Triton X-100. Triton X-100-solubilized samples were added to mAb 1H4-coated wells of 96-well microtitre ELISA plates, previously blocked with 3 % BSA. TBE virus E protein was detected by adding biotinylated MAb 4H8 and HRP-conjugated streptavidin (Sigma). The HRP activity was detected by adding *o*-phenylenediamine dihydrochroride (Sigma) in the presence of 0·03 % H_2O_2.

Immunoprecipitation. 293T cells were transfected with the wild-type or pr63S pCAGprME plasmid as described above. At 24 h post-transfection, the cells were lysed with Triton X-100 in 10 mM TBS, incubated on ice for 20 min and then centrifuged at 16 000 *g* for 20 min. The supernatant, which excluded the nuclear fraction, was precleared on Protein G-Sepharose beads (Amersham Pharmacia Biotech) for 2 h at 4 °C. Precleared lysates were combined with protein G-Sepharose beads with MAb 1H4 and precipitated by incubation for 2 h at 4 °C. Immune complexes were pelleted at 10 000 *g* for 10 s and washed four times with 1 % Triton X-100 in 10 mM TBS. Subsequently, the precipitated materials were solubilized by adding Laemmli buffer (Laemmli, 1970) and by heating to 95 °C for 2 min and then analysed by SDS-PAGE and Western blotting.

SDS-PAGE and Western blotting. Transfected cells were lysed with Laemmli buffer under nonreducing or reducing (in the presence of 2-mercaptoethanol) conditions. Protein samples were electrophoresed through 8 and 15 % polyacrylamide-SDS gels. The protein bands were transferred onto PVDF membranes, then incubated with 1 % gelatin in 25 mM TBS containing 0·01 % Tween 20 (TBST) for 30 min at room temperature. After washing with TBST, the membranes were reacted with polyclonal anti-E or anti-prM rabbit IgG for 1 h, followed by alkaline phosphatase conjugated anti-rabbit IgG (Promega) for 30 min at room temperature. For the detection of glycosylation of envelope proteins, the membranes were treated with biotin conjugated concanavalin A (Honen Corporation) and then with alkaline phosphatase conjugated streptavidin (Sigma). Protein bands were visualized using the AP detection reagent kit (Novagen).

Immunofluorescence assay. 293T cells grown on eight-well chamber slides (Nalge Nunc International) were transfected with the wild-type or pr63S pCAGprME plasmids. At 8 h post-transfection, cells were rinsed with PBS and fixed with 4 % paraformaldehyde for 10 min, then permeabilized with 0·2 % Triton X-100 for 4 min at room temperature. After blocking with 2 % BSA for 30 min, the cells were incubated at room temperature for 1 h with mouse mAb 1H4 and antibodies that recognize marker proteins of various cellular organelles, at dilutions between 1:100 and 1:1000 in antibody-dilution buffer (PBS containing 0·1 % Triton X-100 and 2 mg BSA ml^{-1}). After extensive washing, the cells were incubated at room temperature for 1 h with fluorescence-label conjugated secondary antibodies, diluted 1:200. The cells were washed three times with PBS, followed by mounting of the coverslips on glass slides. Images were viewed and collected with an Olympus IX70 confocal microscope.

Electron microscopy. 293T cells were transfected with the wild-type or pr63S pCAGprME plasmids. At 24 h post-transfection, cells were harvested and centrifuged at 1000 *g* for 5 min. The pellets were fixed with 3 % (v/v) glutaraldehyde in 0·1 M phosphate buffer (pH 7·2) for 3 h and then rinsed three times with 0·1 M phosphate buffer. After post-fixation in a 1 % (w/v) osmium tetraoxide solution for 1·5 h, the pellets were dehydrated through a series of graded ethanols and embedded in Epon 812 via QY1 (Nishin EM). Ultrathin sections were cut, stained with uranyl acetate and lead citrate, and examined under a JEM 1210 transmission electron microscope (JEOL) at an acceleration voltage of 80 kV.

RNA transcription and transfection. Oshima IC-pt or Oshima IC-pr63S were digested with *Spe*I and extracted using a QIAquick gel extraction kit (Qiagen). Infectious RNA was transcribed *in vitro* using mMESSAGE mMACHINE SP6 kits (Ambion) in 20 μl reaction volumes, with an additional 1 μl GTP solution. After the transcription at 37 °C for 2 h, template DNA was removed by DNase I digestion 37 °C for 15 min. RNA was precipitated with lithium chloride, washed with 70 % ethanol, resuspended in RNase-free water, and stored in aliquots at −80 °C.

Approximately 5×10^6 BHK cells in 0·5 ml cold PBS were electroporated with 10 μg RNA in 0·4 cm cuvettes using a GenePulser apparatus (Bio-Rad), pulsing twice at settings of 1·3 kV, 25 μF and maximum resistance. Transfected cells were equally divided into two T-25 flasks. After an overnight recovery, cell debris resulting from electroporation was washed away twice with PBS and fresh medium was added. At various times post-electroporation, aliquots of media were harvested as a source of recovered viruses. Infectious virus titre was assayed by the focus count assay, as described previously (Takashima *et al.*, 1997).

RESULTS

Mutant plasmid which induces a reduction of secretion of VLPs

We previously constructed plasmid pCAGprME, which expresses recombinant TBE virus prM/E proteins (Yoshii *et al.*, 2003). In this system, VLPs are secreted from pCAGprME-transfected cells. In the current study, a mutant plasmid, which induced suppression of VLP secretion in spite of higher levels of intracellular viral proteins, was obtained by error-prone PCR. 293T cells were transfected with pCAGprME wild-type or with the mutant clone, designated clone 55. Although higher levels of E proteins were detected from cell lysates transfected with the mutant clone 55 by ELISA, E proteins in the culture media were drastically reduced (to approximately 1/50 to 1/100), as compared with the media of cells transfected with the wild-type plasmid.

Complete sequencing of the pCAGprME mutant clone 55 allowed identification of 5 nt changes that induce 4 aa changes (Fig. 1). The mutant prM protein had 2 aa changes at positions 63 and 88 in the pr region, which was eventually removed by an intracellular furin protease to produce the

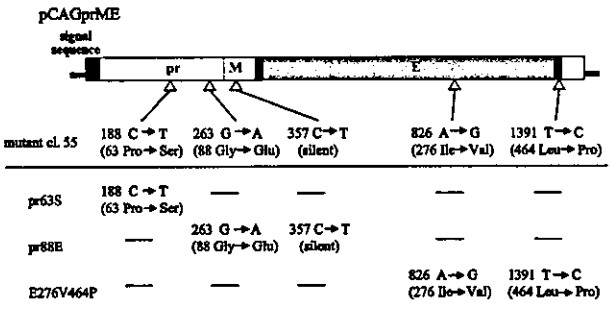

Fig. 1. Schematic representation of the plasmids encoding various parts of TBE virus prM and E proteins. The signal sequence domain and transmembrane regions of prM and E are shown as black boxes. Positions of the mutations in the mutant plasmids used in this study were indicated by open triangles. Numbers of nucleotides and amino acids starting from the amino terminus of prM and E protein according to TBE virus Oshima 5-10 strain genomic sequence (GenBank accession no. AB062063).

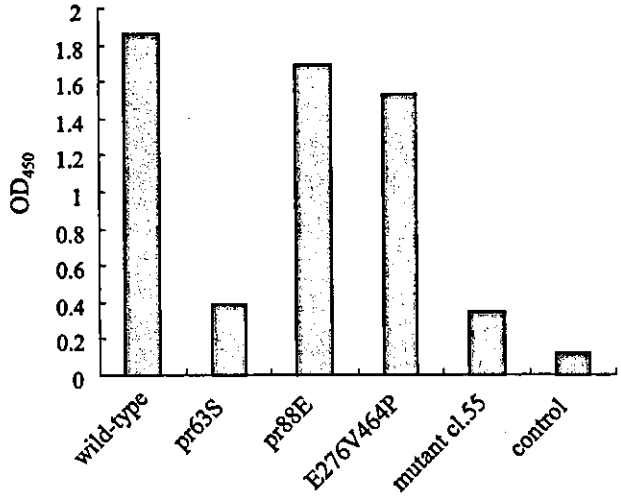

Fig. 2. Identification of the mutation that induces the suppression of VLP secretion. 293T cells were transfected with pCAGprME wild-type, pr63S, pr88E, E276B464P, mutant clone 55 and control plasmid pCAGGS. At 24 h post-transfection, culture media were collected and treated with Triton X-100. E protein in solubilized samples was detected by ELISA using TBE virus E-protein-specific mAb.

mature M protein (Stadler *et al.*, 1997). The mutant E protein had two amino acid changes at positions 276 and 464. The Ile→Val substitution at position 276 is a conservative amino acid change and maps to the domain II of E proteins (Rey *et al.*, 1995). The Leu→Pro substitution at position 464 maps to the first transmembrane region of E protein, which constitutes a membrane anchor (Allison *et al.*, 1999; Mandl *et al.*, 1989; Rice, 1996).

Identification of mutation involved in the reduction of secretion of VLPs

To determine which of the mutations was involved in the reduction of secretion of VLPs, three plasmids were constructed (Fig. 1): pCAGprME pr63S, containing a Pro→Ser mutation at position 63 in prM; pr88E, containing a Gly→Glu mutation at position 88 in prM; and E276V464P, containing Ile→Val and Leu→Pro mutations at positions 276 and 464 in E protein. We then transfected 293T cells with pCAGprME wild-type, mutant clone 55, pr63S, pr88E and E276V464P. At 24 h post-transfection, the culture media were harvested and E protein was detected by ELISA, as described above. Cells transfected with pr88E and E276V464P secreted the same level of E protein as wild-type-transfected cells, but pr63S-transfected cells secreted very low levels of E protein, as did mutant-clone-55-transfected cells (Fig. 2). This indicated that the Pro→Ser mutation at position 63 in prM protein was involved in the reduction of VLP secretion.

To compare the kinetics of protein E secretion from cells transfected with pCAGprME wild-type and pr63S, supernatant and cell lysate samples were collected at 6, 9, 12, 16, 20, 24 and 28 h post-transfection. Levels of protein E in the intracellular and extracellular fractions were detected by ELISA. Regardless of prM mutation, almost equivalent level of protein E was detected by monoclonal antibodies that recognize conformational structures of protein E (Fig. 3a), indicating that prM mutation did not disturb protein E from reaching its final conformational structure. However, protein E secretion was drastically reduced by the prM mutation (Fig. 3b). This indicated that protein E, which was not effectively secreted from mutant-transfected cells, accumulated intracellularly.

Interaction between prM and E proteins

PrM and E proteins form heterodimers, which are involved in the folding and maturation of E protein (Konishi & Mason, 1993; Lorenz *et al.*, 2002). To examine the mechanism of the reduction of secretion of VLPs induced by the Pro→Ser mutation at position 63 in prM protein, we first investigated the interaction between prM and E proteins. To investigate the heterodimer formation of prM and E protein, 293T cells transfected with the wild-type or the pr63S pCAGprME plasmid were lysed with Triton X-100, and the post-nuclear supernatants were immunoprecipitated with anti-E-specific mAb 1H4 (Komoro *et al.*, 2000). Immunoprecipitates were then separated by SDS-PAGE and protein bands were detected by anti-E and anti-prM rabbit IgG, as described in Methods. As shown in Fig. 4(a), prM proteins were detected from immunoprecipitated samples from pr63S-transfected cells as well as from wild-type-transfected cells. The intensities for prM and E bands of pr63S-transfected cells were higher than those of wild-type-transfected cells, as observed in Fig. 3. These data indicated that heterodimerization between prM and E had occurred in spite of prM mutation. The glycosylation of prM and E proteins was examined by concanavalin A, which

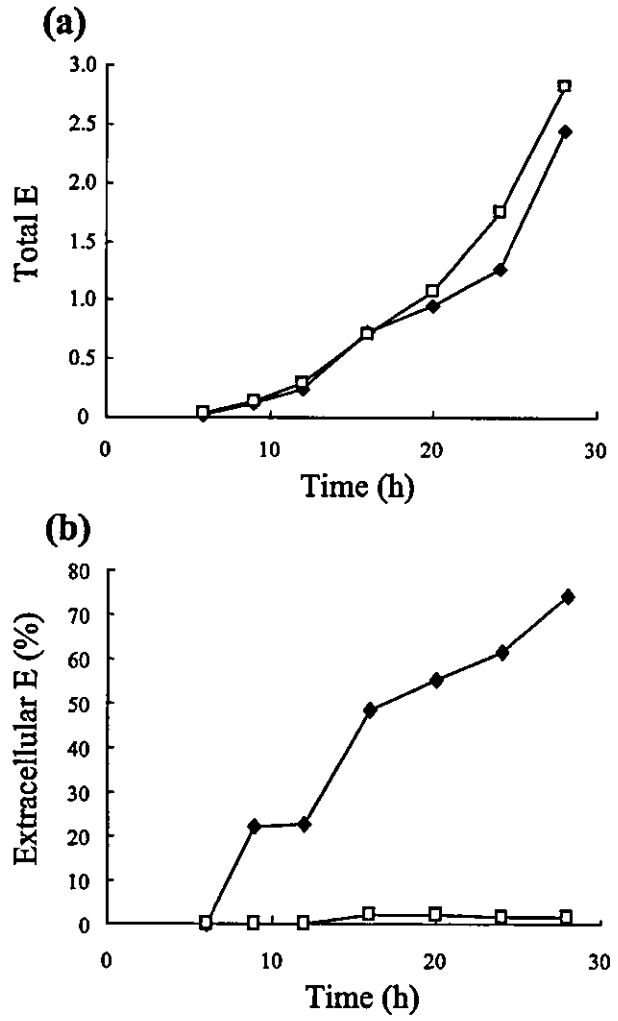

Fig. 3. Time course of protein E expression and secretion. Intracellular and extracellular extracts of 293T cells transfected with pCAGprME wild-type (closed diamond) or pr63S (open square) were collected at 6, 9, 12, 16, 20, 24 or 28 h post-transfection and E protein expression was quantified by ELISA. (a) To calculate total amount of E protein (intracellular and extracellular fractions), E expressed from wild-type-transfected cells at 20 h was set at 1·0. (b) Percentage of total E protein in the extracellular fraction.

binds to *N*-linked glycan. PrM and E proteins were glycosylated well in the immunoprecipitated sample of pr63S-transfected cells, indicating that the two proteins were functionally glycosylated. The effect of Pro→Ser mutation in prM proteins on oxidative folding were further analysed by SDS-PAGE under reducing and nonreducing conditions (Fig. 4b). For prM, a clear difference in the electrophoretic mobility between nonreducing and reducing conditions was visible. This shift was identical for wild-type and mutant samples, indicating that disulfide bond formation occurred normally even in the presence of prM mutation. The corresponding shift in the E protein band was much smaller but was consistently observed regardless of prM mutation. These data showed that the Pro→Ser mutation at position 63 in the prM protein did not affect the interaction and folding of prM and E proteins, regardless of the observed reduction in VLP secretion.

Intracellular localization of recombinant TBE virus envelope proteins

To determine the intracellular distribution of the viral envelope proteins, 293T cells were transfected with pCAGprME wild-type or pr63S plasmids. The cells were fixed, permeabilized and double stained for TBE virus envelope proteins and cellular marker antigens. Anti-calreticulin (Michalak *et al.*, 1992) was used as a marker for ER (Fig. 5b and e), and anti-giantin (Linstedt & Hauri, 1993) was used as a marker for the Golgi complex (Fig. 5h and k). A mouse mAb anti-E (Fig. 5a, d, g and j) was used to stain viral envelope proteins. In wild-type-transfected cells, the distribution of viral envelope protein overlapped almost completely with the ER marker (Fig. 5c) and Golgi marker (Fig. 5i), indicating that viral envelope protein was transported into the Golgi complex. While distribution of viral envelope protein in the ER was observed (Fig. 5f), overlap of viral envelope proteins and Golgi marker was hardly seen in pr63S-transfected cells (Fig. 5l). These data suggest that the mutation at position 63 in prM proteins causes the accumulation of viral envelope proteins in the ER.

Electron microscopy analysis of VLP assembly

As shown in Fig. 6(a), many VLPs were observed in the lumen of the ER in wild-type-transfected cells. However, in pr63S-transfected cells, the spherical VLPs observed in wild-type-transfected cells were hardly seen in the ER lumen; instead, there were many long tubular structures in the ER lumen (Fig. 6b). The tubular particles were 0·1 to 2·0 μm in length and they were not observed in the Golgi complex (data not shown).

Pro→Ser mutation in prM protein affects TBEV infectivity

To investigate the effect of the prM mutation on viral infectivity or on viral budding, the Pro→Ser mutation at position 63 was inserted into an infectious cDNA clone of the TBE virus genome. A full-length TBE viral cDNA containing Pro→Ser mutation was constructed (Oshima IC-pr63S), and BHK cells were transfected with *in vitro*-transcribed TBE viral RNA. Virus production was analysed by focus count assay of the medium harvested from transfected cells at 24 and 48 h post-transfection. As shown in Table 2, the cells transfected with Oshima IC-pr63S secreted fewer infective virus particles than cells transfected with Oshima IC-pt. Total secreted E proteins were also reduced by Pro→Ser mutation and secreted E proteins to f.f.u. ratios were almost same regardless of prM mutation. There was no mutation in recovered virus except for Pro→Ser mutation in prM. These data confirm the

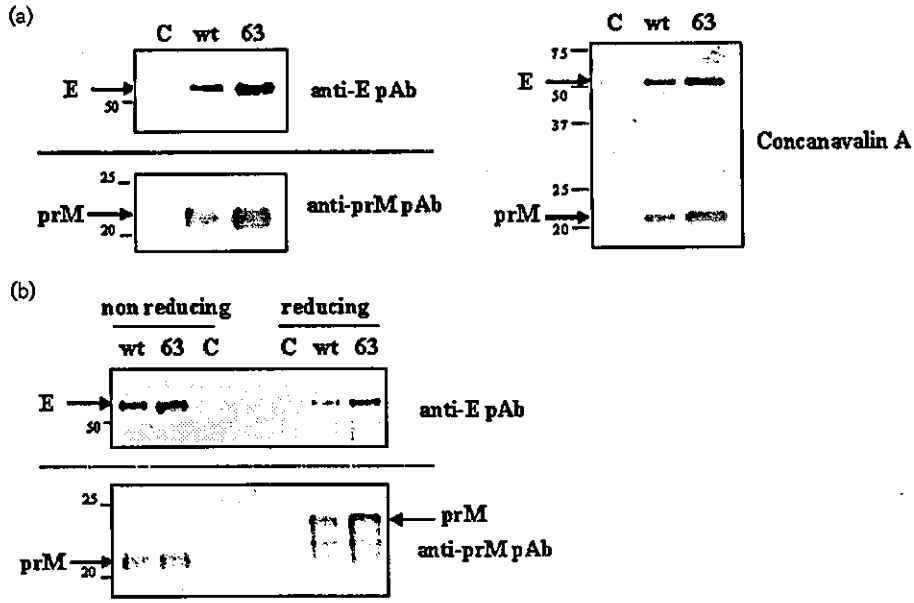

Fig. 4. Interaction between prM and E proteins expressed in transfected 293T cells. (a) Heterodimer formation of prM and E proteins in transfected cells. 293T cells were transfected with pCAGprME wild-type (wt), pr63S (63) or control plasmid pCAGGS (C). At 24 h post-transfection, post-nuclear supernatant was immunoprecipitated with mouse anti-E mAb 1H4, followed by analysis of the proteins by SDS-PAGE (7·5 and 12%, top and bottom, respectively), and transferred to PVDF membranes. Protein bands were detected using anti-E and anti-prM rabbit polyclonal antiserum. Concanavalin A was used for the detection of glycosylated proteins. Positions of the individual proteins are marked, and molecular size is indicated at the side, in kilodaltons. (b) Oxidative folding of prM and E in transfected cells. Post-nuclear supernatant of transfected cells was subjected to SDS-PAGE in nonreducing and reducing conditions and transferred to membrane. Protein bands were detected using anti-E and anti-prM rabbit polyclonal antiserum.

findings of the expression studies concerning the effects of the pr63S mutation on secretion of TBE virus VLPs.

DISCUSSION

In many enveloped viruses, the envelope proteins play important roles in the assembly and budding of virus particles (Garoff *et al.*, 1998). In flaviviruses, it has been shown that virus envelope proteins prM and E are secreted in the form of VLPs when they are expressed recombinantly in mammalian cells without other viral proteins (Allison *et al.*, 1995b; Konishi *et al.*, 1992). Because VLPs have features that are structurally and functionally similar to virus envelope, they have been used as useful tools in the investigation of virus envelope function and the kinetics of viral envelope proteins (Allison *et al.*, 2001; Corver *et al.*, 2000; Lorenz *et al.*, 2003; Op De Beeck *et al.*, 2003). In this study, we constructed a mutant plasmid that reduced VLP secretion in cells expressing recombinant TBE virus prM and E proteins. By analysis of the mutant plasmids, the Pro→Ser mutation at position 63 of the prM protein was found to cause the reduced VLP secretion (Fig. 2). PrM has been reported to serve as a chaperone-like protein in the early steps of virus maturation (Konishi & Mason, 1993; Lorenz *et al.*, 2002). After the cleavage of an N-terminal signal sequence of prM by a host cellular peptidase, prM forms heterodimers with E protein, and E protein attains its native conformation (Stocks & Lobigs, 1995). In addition, it has been thought that prM protects E protein from low-pH rearrangements during transport thorough the acidic compartments of the *trans*-Golgi network by keeping E protein in an inactive structure (Heinz & Allison, 2000). To date, the function of prM in E protein maturation has been studied, but other properties of prM are still unclear. Consequently, this mutation in prM, which reduces VLP secretion, brings a new aspect to the study of prM functions.

The interaction between prM and E proteins is important during the early events of virus particle maturation and secretion. It has been reported that E protein cannot attain full maturity when expressed alone, while prM protein is able to fold independently of other viral components (Lorenz *et al.*, 2002). Furthermore, the secretion of E protein requires cosynthesis with prM, as demonstrated previously in many flaviviruses (Allison *et al.*, 1995b; Konishi & Mason, 1993; Ocazionez Jimenez & Lopes da Fonseca, 2000). Heterodimerization of prM and E leads to the final native conformation of E protein, which is an early process in virus maturation. Therefore, we first examined whether the reduced VLP secretion induced by the position 63 mutation in prM was related to the alteration of interaction between the prM and E proteins. The results of immunoprecipitation

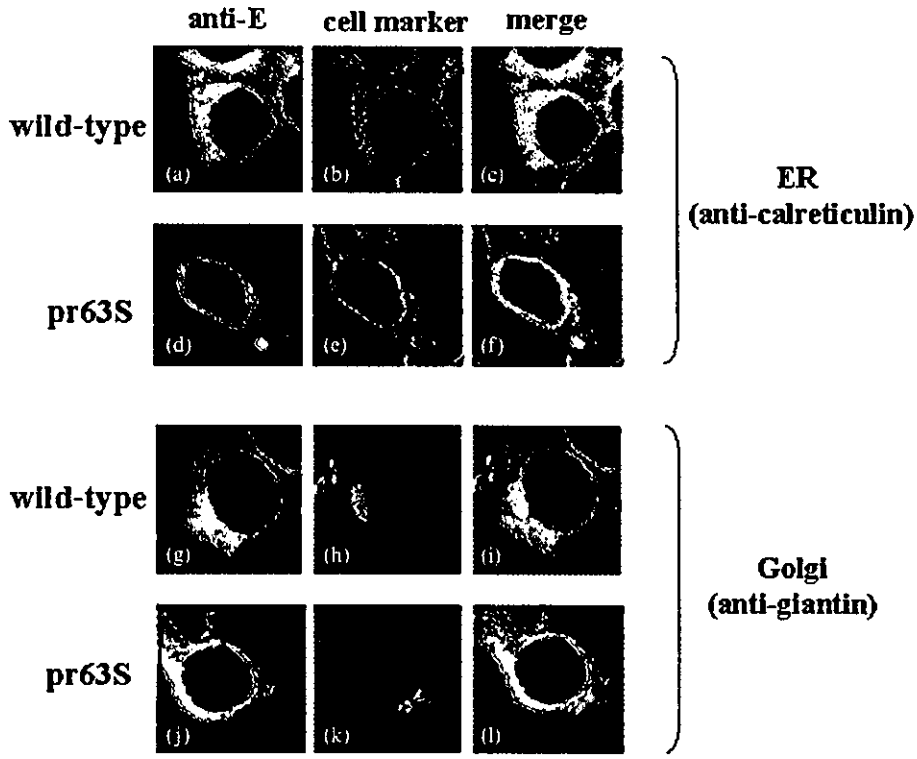

Fig. 5. Intracellular localization of expressed envelope proteins. 293T cells transfected with pCAGprME wild-type (a, b, c, g, h and i) or pr63S (d, e, f, j, k and l) were fixed and subjected to dual staining with TBE virus-specific antibodies and antibodies against marker proteins for cellular organelles as primary antibodies. The samples were then reacted with secondary antibodies conjugated to FITC or Texas red. Shown are cells stained with a mouse anti-E mAb 1H4 (a, d, g and j), immunofluorescent staining of ER with rabbit polyclonal anti-calreticulin (b and e) and immunostaining of the Golgi with rabbit polyclonal anti-giantin antibodies (h and k). Colocalization of viral envelope protein with organelle markers is represented by the yellow regions within each cell in the merged images (c, f, i and l).

with anti-E monoclonal antibodies also indicate that heterodimerization between prM and E, as well as oxidative folding and glycosylation of viral envelope proteins, occurred normally in the presence of the position 63 mutation in prM (Fig. 4). Furthermore, total production level of protein E, which had conformational structures, was not affected by the prM mutation (Fig. 3a), indicating that the position-63 mutation in prM does not detrimentally affect the maturation of protein E. These data suggest that the reduction of VLP secretion induced by the prM mutation was due to a later step of virus particle budding and secretion, not to the prM and E interaction in the early events of virus budding.

It has been reported that flavivirus particles are assembled into the ER lumen (Mackenzie & Westaway, 2001). Thus, the mechanism of flavivirus secretion can be divided into two steps. Virus particle budding in ER membrane, followed by virus transport through the secretory pathway. To identify the influence of the prM position 63 mutation in virus secretion, the intracellular localization of the viral envelope proteins was examined. Envelope proteins expressed with the mutated prM were not transported to the Golgi complex, and accumulated in the ER (Fig. 5). Electron microscopic analysis revealed that many tubular structures, which differed from spherical VLPs in shape, were observed in the ER lumen of cells transfected with a plasmid, with the mutation in prM (Fig. 6). In the Lorenz *et al.* (2003) study, it was reported that similar tubular structures were occasionally seen in cells expressing TBE virus prM and E, and that these structures were not observed in the Golgi complex. The tubular structures observed in cells expressing mutated prM and E in our study may be comparable to those noted in the Lorenz study, and they may not undergo secretion due to their abnormal budding. Another possibility is that the tubular structures are membrane components that detach from the ER lumen due to the damage to membrane structures caused by accumulation of viral envelope proteins. In any case, the position 63 mutation in prM clearly affects the budding process of the virus particle.

In many enveloped viruses, the cytoplasmic domain of the envelope proteins has been assigned an important role in virus assembly. For vesicular stomatitis virus, the cytoplasmic domain is important for incorporation of the

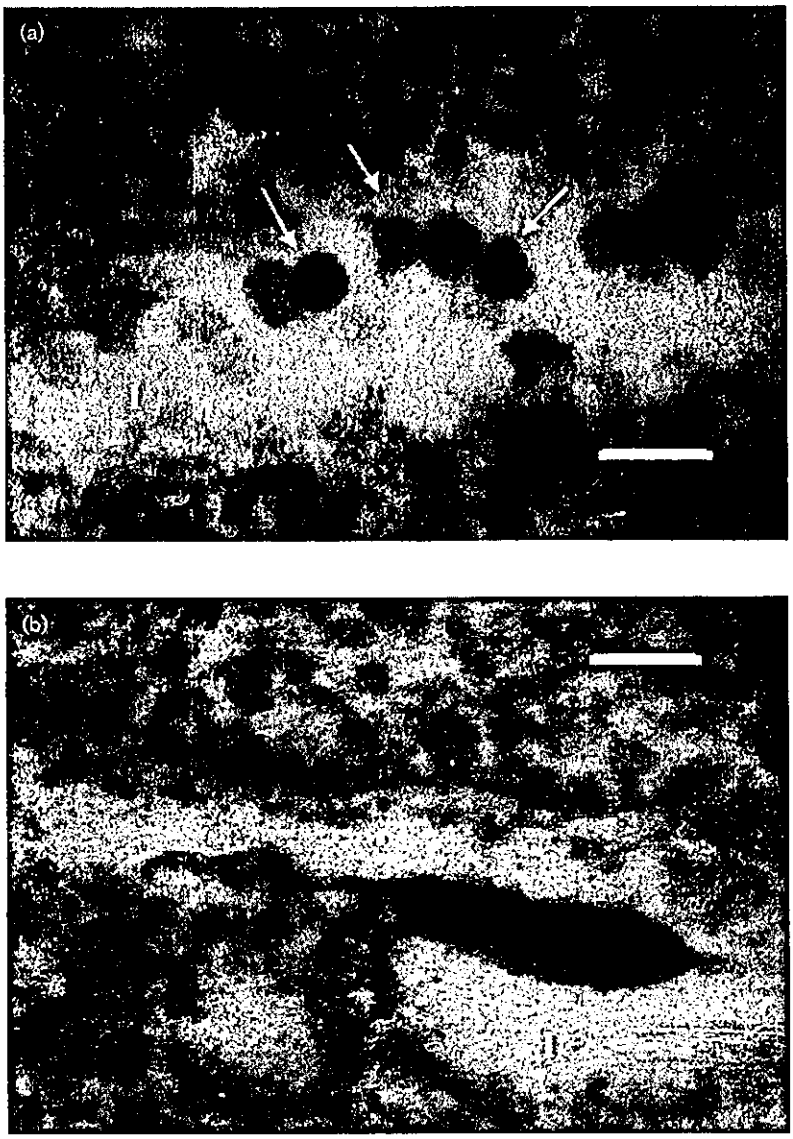

Fig. 6. Electron micrographs of 293T cells transfected with pCAGprME wild-type and pr63S. VLPs (arrow) are seen in the ER lumen of pCAGprME wild-type-transfected cells (a). (b) Shows a long tubular structure (diameter, 120 nm) in the lumen of the ER of pCAGprME pr63S-transfected cells. l, ER lumen. Bars, 50 nm.

glycoprotein (Owens & Rose, 1993; Whitt *et al.*, 1989). For alphaviruses, it has been shown that the cytoplasmic domain of the E2 glycoprotein has a critical role in virus budding (Kail *et al.*, 1991; Owen & Kuhn, 1997; Zhao *et al.*, 1994). Deletion of the cytoplasmic tails of influenza virus haemagglutinin and neuraminidase (NA) leads to irregularly shaped virions, and deletion of the NA cytoplasmic domain reduces the incorporation of NA into virions (Jin *et al.*, 1997; Mitnaul *et al.*, 1996). But unlike these viruses, flavivirus prM and E proteins have cytoplasmic loops consisting of only a few amino acid residues between their two transmembrane segments. Thus, it is

Table 2. Virus titre in media of electroporated BHK-21 cells at 24 and 48 h post-electroporation

Template used for transcription	Virus titre (f.f.u. ml^{-1})		f.f.u./extracellular E*	
	24 h	48 h	24 h	48 h
Oshima IC-pt	$2{\cdot}3 \times 10^5$	$4{\cdot}0 \times 10^6$	1	1·24
Oshima IC-pr63S	$1{\cdot}4 \times 10^4$	$2{\cdot}2 \times 10^5$	0·96	1·29

*Total extracellular E proteins were quantified by ELISA and E proteins to f.f.u. ratios were calculated by setting the ratio of 24 h at 1·0.

thought that the luminal domains, or the two transmembrane domains of prM and E, play more critical roles in the assembly of these viruses.

In a recent study by Zhang *et al.* (2003), the structure of prM-containing immature particles of dengue and yellow fever virus was analysed by cryoelectron microscopy and image reconstruction techniques. The surface of the immature particles was characterized by the presence of 60 fairly prominent projections or spikes, which differed from the smooth surface of mature virus (Kuhn *et al.*, 2002). In the spike structure, prM protein covered the fusion peptides of domain II of the E protein, similar to the case of alphaviruses, where the E2 glycoproteins protect the fusion peptides of the E1 glycoproteins within a trimeric spike (Zhang *et al.*, 2002). Thus, it is suggested that the position 63 mutation in prM may induce conformational changes in the domain exposed on the outer side of the viral envelope, which is important for the virus budding process.

The cellular membranes involved in membrane transport normally form vesicles on the cytoplasmic side, such as clathrin coated vesicles, and COP I and COP II vesicles (Schekman & Orci, 1996). It is possible that prM-E heterodimers, alone or with cellular factors in the ER lumen, assemble laterally and induce the membrane curvature into an isometric lattice, like the assembly of coat proteins in membrane transport vesicles (Keen *et al.*, 1979; Wieland & Harter, 1999). The abnormal budding induced by the prM mutation may be due to a dysfunction in this process, caused by structural changes in prM or by loss of interaction with a cellular component. Alternatively, the prM mutation may be related to the pinching off of particles from the ER membrane, as is the case for dynamin in clathrin-coated vesicles, and it might be possible that VLPs could not be pinched off properly due to the prM mutation (McNiven, 1998).

In summary, by analysis of a prM mutation that induces the reduction of VLP and virus particle secretion, we demonstrated a critical function for prM in the virus budding process. This mutation does not affect the heterodimerization between prM and E, and E proteins can reach the native conformation in spite of the prM mutation, suggesting the preservation of prM's chaperone-like role. Envelope proteins that are not secreted due to the prM mutation accumulate in the ER, indicating the failure of virus particle budding. Molecular approaches focused on the ectodomain of prM protein should enable further investigation of the mechanisms during the virus budding process.

ACKNOWLEDGEMENTS

This work was supported by Grants-in-Aid for Scientific Research, Program of Excellence for Zoonosis Control, and the 21st Century COE Program from the Ministry of Education Science, Sports and Culture of Japan, and Health Sciences Grants for Research from the Ministry of Health, Labor and Welfare of Japan.

REFERENCES

Allison, S. L., Schalich, J., Stiasny, K., Mandl, C. W., Kunz, C. & Heinz, F. X. (1995a). Oligomeric rearrangement of tick-borne encephalitis virus envelope proteins induced by an acidic pH. *J Virol* **69**, 695–700.

Allison, S. L., Stadler, K., Mandl, C. W., Kunz, C. & Heinz, F. X. (1995b). Synthesis and secretion of recombinant tick-borne encephalitis virus protein E in soluble and particulate form. *J Virol* **69**, 5816–5820.

Allison, S. L., Stiasny, K., Stadler, K., Mandl, C. W. & Heinz, F. X. (1999). Mapping of functional elements in the stem-anchor region of tick-borne encephalitis virus envelope protein E. *J Virol* **73**, 5605–5612.

Allison, S. L., Schalich, J., Stiasny, K., Mandl, C. W. & Heinz, F. X. (2001). Mutational evidence for an internal fusion peptide in flavivirus envelope protein E. *J Virol* **75**, 4268–4275.

Corver, J., Ortiz, A., Allison, S. L., Schalich, J., Heinz, F. X. & Wilschut, J. (2000). Membrane fusion activity of tick-borne encephalitis virus and recombinant subviral particles in a liposomal model system. *Virology* **269**, 37–46.

de Haan, C. A., Kuo, L., Masters, P. S., Vennema, H. & Rottier, P. J. (1998). Coronavirus particle assembly: primary structure requirements of the membrane protein. *J Virol* **72**, 6838–6850.

Elshuber, S., Allison, S. L., Heinz, F. X. & Mandl, C. W. (2003). Cleavage of protein prM is necessary for infection of BHK-21 cells by tick-borne encephalitis virus. *J Gen Virol* **84**, 183–191.

Garoff, H., Hewson, R. & Opstelten, D. J. (1998). Virus maturation by budding. *Microbiol Mol Biol Rev* **62**, 1171–1190.

Gritsun, T. S., Lisak, V. M., Liapustin, V. N., Korolev, M. B. & Lashkevich, V. A. (1989). Slowly-sedimenting hemagglutinin of the tick-borne encephalitis virus. *Vopr Virusol* **34**, 449–454 (in Russian).

Hayasaka, D., Gritsun, T. S., Yoshii, K. & 7 other authors (2004). Amino acid changes responsible for attenuation of virus neurovirulence in an infectious cDNA clone of the Oshima strain of *Tick-borne encephalitis virus*. *J Gen Virol* **85**, 1007–1018.

Heinz, F. & Kunz, C. (1977). Concentration and purification of tick-borne encephalitis virus grown in suspensions of chick embryo cells. *Acta Virol* **21**, 301–307.

Heinz, F. X. & Mandl, C. W. (1993). The molecular biology of tick-borne encephalitis virus. Review article. *APMIS* **101**, 735–745.

Heinz, F. X. & Allison, S. L. (2000). Structures and mechanisms in flavivirus fusion. *Adv Virus Res* **55**, 231–269.

Ishak, R., Tovey, D. G. & Howard, C. R. (1988). Morphogenesis of yellow fever virus 17D in infected cell cultures. *J Gen Virol* **69**, 325–335.

Jin, H., Leser, G. P., Zhang, J. & Lamb, R. A. (1997). Influenza virus hemagglutinin and neuraminidase cytoplasmic tails control particle shape. *EMBO J* **16**, 1236–1247.

Kail, M., Hollinshead, M., Ansorge, W., Pepperkok, R., Frank, R., Griffiths, G. & Vaux, D. (1991). The cytoplasmic domain of alphavirus E2 glycoprotein contains a short linear recognition signal required for viral budding. *EMBO J* **10**, 2343–2351.

Keen, J. H., Willingham, M. C. & Pastan, I. H. (1979). Clathrin-coated vesicles: isolation, dissociation and factor-dependent reassociation of clathrin baskets. *Cell* **16**, 303–312.

Komoro, K., Hayasaka, D., Mizutani, T., Kariwa, H. & Takashima, I. (2000). Characterization of monoclonal antibodies against Hokkaido strain tick-borne encephalitis virus. *Microbiol Immunol* **44**, 533–536.

Konishi, E. & Mason, P. W. (1993). Proper maturation of the Japanese encephalitis virus envelope glycoprotein requires cosynthesis with the premembrane protein. *J Virol* **67**, 1672–1675.

Konishi, E., Pincus, S., Paoletti, E., Shope, R. E., Burrage, T. & Mason, P. W. (1992). Mice immunized with a subviral particle containing the Japanese encephalitis virus prM/M and E proteins are protected from lethal JEV infection. *Virology* **188**, 714–720.

Kuhn, R. J., Zhang, W., Rossmann, M. G. & 9 other authors (2002). Structure of dengue virus: implications for flavivirus organization, maturation, and fusion. *Cell* **108**, 717–725.

Laemmli, U. K. (1970). Cleavage of structural proteins during the assembly of the head of bacteriophage T4. *Nature* **227**, 680–685.

Lindenbach, B. D. & Rice, C. M. (2001). *Flaviviridae*: the viruses and their replication. In *Fields Virology*, 4th edn, pp. 991–1041. Edited by D. M. Knipe & P. M. Howley. Philadelphia: Lippincott Williams & Wilkins.

Linstedt, A. D. & Hauri, H. P. (1993). Giantin, a novel conserved Golgi membrane protein containing a cytoplasmic domain of at least 350 kDa. *Mol Biol Cell* **4**, 679–693.

Lorenz, I. C., Allison, S. L., Heinz, F. X. & Helenius, A. (2002). Folding and dimerization of tick-borne encephalitis virus envelope proteins prM and E in the endoplasmic reticulum. *J Virol* **76**, 5480–5491.

Lorenz, I. C., Kartenbeck, J., Mezzacasa, A., Allison, S. L., Heinz, F. X. & Helenius, A. (2003). Intracellular assembly and secretion of recombinant subviral particles from tick-borne encephalitis virus. *J Virol* **77**, 4370–4382.

Mackenzie, J. M. & Westaway, E. G. (2001). Assembly and maturation of the flavivirus Kunjin virus appear to occur in the rough endoplasmic reticulum and along the secretory pathway, respectively. *J Virol* **75**, 10787–10799.

Mandl, C. W., Guirakhoo, F., Holzmann, H., Heinz, F. X. & Kunz, C. (1989). Antigenic structure of the flavivirus envelope protein E at the molecular level, using tick-borne encephalitis virus as a model. *J Virol* **63**, 564–571.

Mason, P. W., Pincus, S., Fournier, M. J., Mason, T. L., Shope, R. E. & Paoletti, E. (1991). Japanese encephalitis virus-vaccinia recombinants produce particulate forms of the structural membrane proteins and induce high levels of protection against lethal JEV infection. *Virology* **180**, 294–305.

McNiven, M. A. (1998). Dynamin: a molecular motor with pinchase action. *Cell* **94**, 151–154.

Michalak, M., Milner, R. E., Burns, K. & Opas, M. (1992). Calreticulin. *Biochem J* **285**, 681–692.

Mitnaul, L. J., Castrucci, M. R., Murti, K. G. & Kawaoka, Y. (1996). The cytoplasmic tail of influenza A virus neuraminidase (NA) affects NA incorporation into virions, virion morphology, and virulence in mice but is not essential for virus replication. *J Virol* **70**, 873–879.

Niwa, H., Yamamura, K. & Miyazaki, J. (1991). Efficient selection for high-expression transfectants with a novel eukaryotic vector. *Gene* **108**, 193–199.

Ocazionez Jimenez, R. & Lopes da Fonseca, B. A. (2000). Recombinant plasmid expressing a truncated dengue-2 virus E protein without co-expression of prM protein induces partial protection in mice. *Vaccine* **19**, 648–654.

Op De Beeck, A., Molenkamp, R., Caron, M., Ben Younes, A., Bredenbeek, P. & Dubuisson, J. (2003). Role of the transmembrane domains of prM and E proteins in the formation of yellow fever virus envelope. *J Virol* **77**, 813–820.

Owen, K. E. & Kuhn, R. J. (1997). Alphavirus budding is dependent on the interaction between the nucleocapsid and hydrophobic amino acids on the cytoplasmic domain of the E2 envelope glycoprotein. *Virology* **230**, 187–196.

Owens, R. J. & Rose, J. K. (1993). Cytoplasmic domain requirement for incorporation of a foreign envelope protein into vesicular stomatitis virus. *J Virol* **67**, 360–365.

Patzer, E. J., Nakamura, G. R., Simonsen, C. C., Levinson, A. D. & Brands, R. (1986). Intracellular assembly and packaging of hepatitis B surface antigen particles occur in the endoplasmic reticulum. *J Virol* **58**, 884–892.

Rey, F. A., Heinz, F. X., Mandl, C., Kunz, C. & Harrison, S. C. (1995). The envelope glycoprotein from tick-borne encephalitis virus at 2 A resolution. *Nature* **375**, 291–298.

Rice, C. M. (1996). *Flaviviridae*: the viruses and their replication. In *Fields Virology*, 3rd edn, pp. 931–959. Edited by B. N. Fields, D. N. Knipe, P. M. Howley, R. M. Chanock, J. L. Melnick, T. P. Monath, B. Roizman & S. E. Straus. Philadelphia: Lippincott-Raven.

Schekman, R. & Orci, L. (1996). Coat proteins and vesicle budding. *Science* **271**, 1526–1533.

Simon, K., Lingappa, V. R. & Ganem, D. (1988). Secreted hepatitis B surface antigen polypeptides are derived from a transmembrane precursor. *J Cell Biol* **107**, 2163–2168.

Stadler, K., Allison, S. L., Schalich, J. & Heinz, F. X. (1997). Proteolytic activation of tick-borne encephalitis virus by furin. *J Virol* **71**, 8475–8481.

Stiasny, K., Allison, S. L., Mandl, C. W. & Heinz, F. X. (2001). Role of metastability and acidic pH in membrane fusion by tick-borne encephalitis virus. *J Virol* **75**, 7392–7398.

Stiasny, K., Allison, S. L., Schalich, J. & Heinz, F. X. (2002). Membrane interactions of the tick-borne encephalitis virus fusion protein E at low pH. *J Virol* **76**, 3784–3790.

Stocks, C. E. & Lobigs, M. (1995). Posttranslational signal peptidase cleavage at the flavivirus C-prM junction in vitro. *J Virol* **69**, 8123–8126.

Takashima, I., Morita, K., Chiba, M. & 8 other authors (1997). A case of tick-borne encephalitis in Japan and isolation of the virus. *J Clin Microbiol* **35**, 1943–1947.

Vennema, H., Godeke, G. J., Rossen, J. W., Voorhout, W. F., Horzinek, M. C., Opstelten, D. J. & Rottier, P. J. (1996). Nucleocapsid-independent assembly of coronavirus-like particles by co-expression of viral envelope protein genes. *EMBO J* **15**, 2020–2028.

Wang, J. J., Liao, C. L., Chiou, Y. W., Chiou, C. T., Huang, Y. L. & Chen, L. K. (1997). Ultrastructure and localization of E proteins in cultured neuron cells infected with Japanese encephalitis virus. *Virology* **238**, 30–39.

Wengler, G. & Wengler, G. (1989). Cell-associated West Nile flavivirus is covered with E+pre-M protein heterodimers which are destroyed and reorganized by proteolytic cleavage during virus release. *J Virol* **63**, 2521–2526.

Whitt, M. A., Chong, L. & Rose, J. K. (1989). Glycoprotein cytoplasmic domain sequences required for rescue of a vesicular stomatitis virus glycoprotein mutant. *J Virol* **63**, 3569–3578.

Wieland, F. & Harter, C. (1999). Mechanisms of vesicle formation: insights from the COP system. *Curr Opin Cell Biol* **11**, 440–446.

Yoshii, K., Hayasaka, D., Goto, A. & 8 other authors (2003). Enzyme-linked immunosorbent assay using recombinant antigens expressed in mammalian cells for serodiagnosis of tick-borne encephalitis. *J Virol Methods* **108**, 171–179.

Zhang, W., Mukhopadhyay, S., Pletnev, S. V., Baker, T. S., Kuhn, R. J. & Rossmann, M. G. (2002). Placement of the structural proteins in Sindbis virus. *J Virol* **76**, 11645–11658.

Zhang, Y., Corver, J., Chipman, P. R. & 7 other authors (2003). Structures of immature flavivirus particles. *EMBO J* **22**, 2604–2613.

Zhao, H., Lindqvist, B., Garoff, H., von Bonsdorff, C. H. & Liljestrom, P. (1994). A tyrosine-based motif in the cytoplasmic domain of the alphavirus envelope protein is essential for budding. *EMBO J* **13**, 4204–4211.

Arch Virol (2004) 149: 1373–1382
DOI 10.1007/s00705-003-0285-4

Archives of Virology
Printed in Austria

Age-dependent hantavirus-specific CD8$^+$ T-cell responses in mice infected with Hantaan virus

K. Araki[1], K. Yoshimatsu[2], B.-H. Lee[2], M. Okumura[2], H. Kariwa[1], I. Takashima[1], and J. Arikawa[2]

[1]Laboratory of Public Health, Department of Environmental Veterinary Sciences, Graduate School of Veterinary Medicine, Hokkaido University, Sapporo, Japan
[2]Institute for Animal Experimentation, Graduate School of Medicine, Hokkaido University, Sapporo, Japan

Received October 9, 2003; accepted December 1, 2003
Published online March 5, 2004

Summary. To investigate age-dependent differences in hantavirus-specific CD8$^+$ T-cell responses, mice were inoculated with 0.1 50% newborn mouse lethal dose of Hantaan virus (HTNV) at 0, 3, 7, 14, or 35 days after birth. HTNV-specific CD8$^+$ T cells producing gamma interferon (IFN-γ) were measured on day 30 after HTNV inoculation. Although no IFN-γ-producing HTNV-specific CD8$^+$ T cells were detected in most of the mice inoculated with HTNV on day 0 after birth, most mice inoculated at 3, 7, 14, or 35 days had HTNV-specific CD8$^+$ T cells. The production of tumor necrosis factor alpha (TNF-α) by IFN-γ-producing CD8$^+$ T cells and the cytotoxic activity against HTNV-infected target cells were similar in immature and adult mice. However, the number of IFN-γ-producing HTNV-specific CD8$^+$ T cells was significantly less in mice inoculated with HTNV at 3 days than in older mice. In addition, a strong correlation between HTNV persistence and a lack of HTNV-specific CD8$^+$ T cells was observed. These results suggest that mice over 7 days old have the ability to induce functional HTNV-specific CD8$^+$ T-cell responses that are indistinguishable from the responses of adult mice, and that HTNV-specific CD8$^+$ T cells are important for clearance of HTNV.

Introduction

Hantaviruses constitute a genus within the family *Bunyaviridae*. They possess a negative-sense RNA genome that consists of three segments. The three segments are designated as the large, medium, and small segments, and they encode RNA-dependent RNA polymerase, two glycoproteins (G1 and G2), and nucleocapsid

(N) proteins, respectively [11–13]. Hantaviruses cause two human diseases: hemorrhagic fever with renal syndrome, and hantavirus pulmonary syndrome [10].

Humans become infected with hantaviruses from persistently infected asymptomatic rodent reservoirs [10]. Currently, at least 22 hantavirus species have been identified [4]. In addition, distinct hantaviruses are associated with each rodent species [8].

To investigate the mechanism of persistent hantavirus infection in rodents, in our previous study [2] we established a model of persistent infection by inoculating newborn mice (within 24 h after birth) with a sub-lethal dose of the prototype HTNV strain for the genus *Hantavirus* [16]. Persistently HTNV-infected newborn mice lacked HTNV-specific $CD8^+$ T cells and a strong correlation between the lack of HTNV-specific $CD8^+$ T cells and HTNV persistence was observed. By contrast, in adult mice, HTNV infection was transient and many HTNV-specific $CD8^+$ T cells were induced by infection. However, it remained unclear at what age the shift from newborn- to adult-type HTNV-specific $CD8^+$ T-cell responses occurs. In addition, although studies of rodent $CD8^+$ T-cell responses against hantavirus infection have been done [2, 9], further investigation is necessary to understand hantavirus-specific $CD8^+$ T-cell responses in detail.

In this study, to investigate the differences in HTNV-specific $CD8^+$ T-cell responses between adult and newborn mice and to accumulate knowledge about HTNV-specific $CD8^+$ T-cell responses, mice of different ages (0, 3, 7, 14, and 35 days old) were inoculated with HTNV and HTNV-specific $CD8^+$ T-cell responses were measured on day 30 after HTNV infection.

Materials and methods

Mice

Pregnant and 4-week-old female BALB/c/slc mice were obtained from SLC (Hamamatsu, Japan). All mice were treated according to the laboratory animal control guidelines of our institute, which conform to those of the U.S. National Institute of Health. All experiments were carried out in a class P3 facility.

Viral infection of mice

HTNV cl-1 was obtained by plaque cloning HTNV strain 76-118 [3]. The virus was propagated in the E6 clone of Vero cells in Eagle's minimal essential medium (EME; Invitrogen) supplemented with 5% fetal bovine serum (FBS). BALB/c mice were inoculated subcutaneously (s.c.) with 0.1 50% newborn mouse lethal dose ($NMLD_{50}$) of HTNV, defined as the dose that was lethal for 50% of mice challenged within 24 h after birth. Separate groups of six immature mice were each inoculated on day 0 (within 24 h of birth), 3, 7, or 14 after birth. A group of adult mice was inoculated 35 days after birth.

Detection of cytokine-producing HTNV-specific $CD8^+$ T cells

To detect HTNV-specific $CD8^+$ T cells, we used flow cytometry to assay the intracellular cytokines of $CD8^+$ T cells stimulated by incubation with HTNV-infected antigen-presenting cells, as described previously [2]. Briefly, spleen cells were obtained from mice on day 30 after HTNV inoculation and spleen single-cell suspensions were prepared by homogenizing

the spleens through a mesh. Erythrocytes were lysed with 0.83% NH_4Cl. Spleen cells were added to 96-well round-bottomed plates at a concentration of 5×10^5 cells/well in RPMI 1640 medium supplemented with 10% FBS, 50 μM 2-mercaptoethanol (2-ME), 20 U/ml recombinant interleukin (IL)-2 (Sigma Chemical Co., St. Louis, MO), and 10 μg/ml brefeldin A (Sigma), along with the HTNV-infected or non-infected P388D1 cells at a concentration of 2.5×10^5 cells/ml. After a 6-h incubation, the cells were stained with Tri-color (TC)-conjugated rat anti-mouse CD8a (Ly-2) monoclonal antibody (mAb) (Caltag Laboratories, San Francisco, CA) for 30 min on ice, fixed, and permeabilized with saponin (Sigma), before the addition of fluorescein isothiocyanate-conjugated rat anti-mouse gamma interferon (IFN-γ) mAb (Caltag) and R-phycoerythrin-conjugated rat anti-mouse tumor necrosis factor-alpha (TNF-α) mAb (Caltag). The cell samples were analyzed using the FACSCalibur system (Becton Dickinson), and data analysis was conducted with CellQuest (Becton Dickinson).

Western blotting for the detection of N protein in lungs of HTNV-infected mice

Western blotting was performed using previously published methods [18]. Briefly, lungs were obtained from mice on day 30 after HTNV inoculation and 20 μl of 10% lung homogenate was used as the antigen. Polyclonal rabbit anti-N protein antibody (diluted 1:800 with PBS) [1], prepared by immunizing a rabbit with the truncated N protein expressed in *E. coli*, was used to detect the N protein on the membrane. Horseradish peroxidase-conjugated goat anti-rabbit IgG (1:500, Jackson ImmunoResearch, West Grove, PA) was used as the secondary antibody.

Cytotoxicity assay

The cytotoxicity assay was performed using previously published methods [2]. Briefly, spleen cells were cultured with HTNV in RPMI 1640 medium supplemented with 10% FBS and 50 μM 2-ME for 5 days. Murine IL-2 (20 U/ml; Sigma) was added on day 5 in 1 ml fresh RPMI 1640 medium supplemented with 10% FBS and 50 μM 2-ME, and the spleen cells were incubated for 2 more days. Cultured spleen cells were used as effector cells in the lactate dehydrogenase (LDH) release assay. HTNV-infected P388D1 cells or uninfected P388D1 cells were used as target cells. Spleen cells and target cells were combined in 96-well round-bottomed plates at various effector cell/target cell (E/T) ratios. The plates were incubated at 37 °C in 5% CO_2, and LDH in the supernatant was detected with a cytotoxicity detection kit (Roche). The percent cytotoxicity was calculated, as described in the manufacturer's instructions.

Results

Hantavirus-specific CD8$^+$ T-cell responses

To investigate differences in the HTNV-specific CD8$^+$ T-cell responses of adult and newborn mice, mice were inoculated at 0, 3, 7, 14, or 35 days of age with 0.1 $NMLD_{50}$ of HTNV. CD8$^+$ T-cell responses to HTNV were examined on day 30 after virus inoculation. Although there were few HTNV-specific CD8$^+$ T cells in mice inoculated with HTNV on day 0, HTNV-specific CD8$^+$ T cells were detected in most of the mice inoculated with HTNV on days 3, 7, 14, and 35 after birth (Fig. 1). However, the number of HTNV-specific CD8$^+$ T cells in mice inoculated with HTNV on day 3 was significantly less than in mice inoculated with HTNV

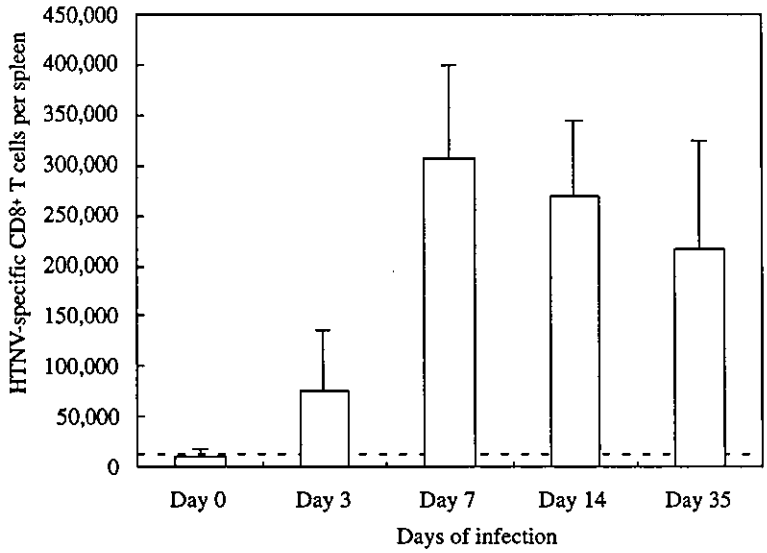

Fig. 1. Immune responses of IFN-γ-producing HTNV-specific $CD8^+$ T cells in HTNV-infected BALB/c mice. Mice were inoculated s.c. with 0.1 $NMLD_{50}$ of HTNV on days 0, 3, 7, 14, or 35 (adult) after birth. Spleen cells were obtained from the HTNV-infected mice on day 30 after virus inoculation. Spleen cells and HTNV-infected P388D1 cells were cocultured at a ratio of 1:0.5 for 6 h in the presence of brefeldin A and IL-2. The number of $CD8^+$ IFN-γ^+ cells per spleen was measured using flow cytometry. Data represent the average numbers from six mice per group. Bars represent the standard deviations. The dotted line indicates the threshold level for detection based on IFN-γ and CD8 staining of spleen cells from naïve mice. No $CD8^+$ IFN-γ^+ cells were detected from a combination of the spleen cells and uninfected P388D1 cells (data not shown)

on days 7, 14, and 35 after birth (Fig. 1, $P < 0.05$). These results show that 7- and 14-day-old mice have the ability to induce HTNV-specific $CD8^+$ T-cell responses that are indistinguishable from the responses of adult mice.

Relationship between HTNV-specific $CD8^+$ T cells and persistence of HTNV

As shown in Fig. 1, HTNV-specific $CD8^+$ T cells were induced in all of the mice inoculated with HTNV at 7, 14, and 35 days of age (individual data not shown), however HTNV-specific $CD8^+$ T-cell responses of mice inoculated with HTNV on days 0 and 3 varied (Fig. 2). A few HTNV-specific $CD8^+$ T cells were observed in one mouse inoculated with HTNV on day 0 after birth (Fig. 2A, f), while no HTNV-specific $CD8^+$ T cells were detected in one mouse inoculated with HTNV on day 3 after birth (Fig. 2B, b); most of the 3-day-old mice had detectable $CD8^+$ T-cell responses.

To examine the persistence of HTNV, we carried out Western blotting for the detection of N protein in the lungs of mice inoculated with HTNV at different ages. Although N protein was detected in all mice inoculated with HTNV on day

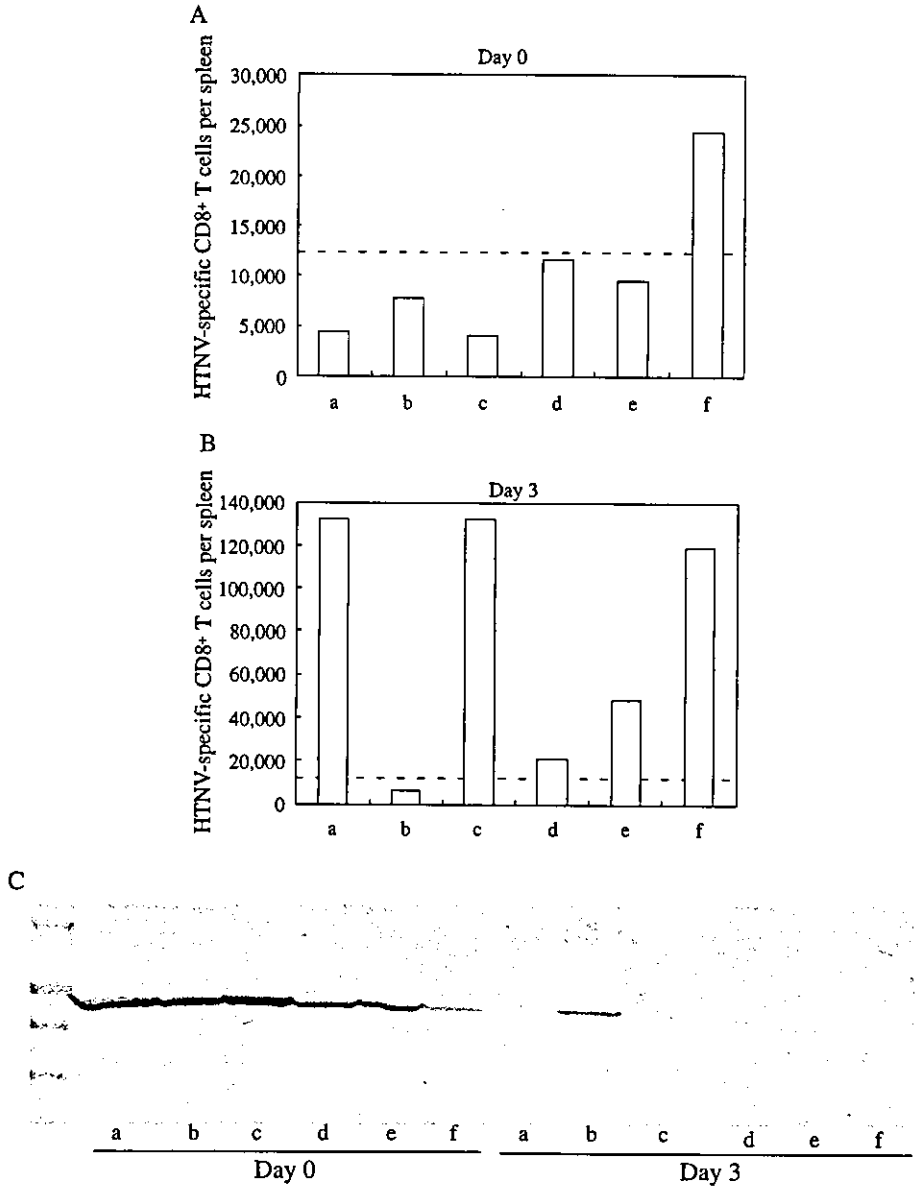

Fig. 2. The number of HTNV-specific CD8$^+$ T cells and N protein content in mice inoculated with HTNV on days 0 and 3 after birth. Data on HTNV-specific CD8$^+$ T cells for each mouse (Days 0 and 3) from Fig. 1 is presented in **A** (Day 0) and **B** (Day 3). The dotted line indicates the threshold level for detection based on IFN-γ and CD8 staining of spleen cells from naïve mice. Lungs were obtained from the HTNV-infected mice on day 30 after virus inoculation. N protein in the lungs was detected by Western blotting (**C**)

0, the amount of N protein was far less in the mouse having HTNV-specific CD8$^+$ T cells (Fig. 2C, Day 0, f). On the other hand, in mice inoculated with HTNV on day 3 after birth, N protein was found only in the mouse in which HTNV-specific CD8$^+$ T cells were not detected (Fig. 2C, Day 3, b). In mice inoculated with

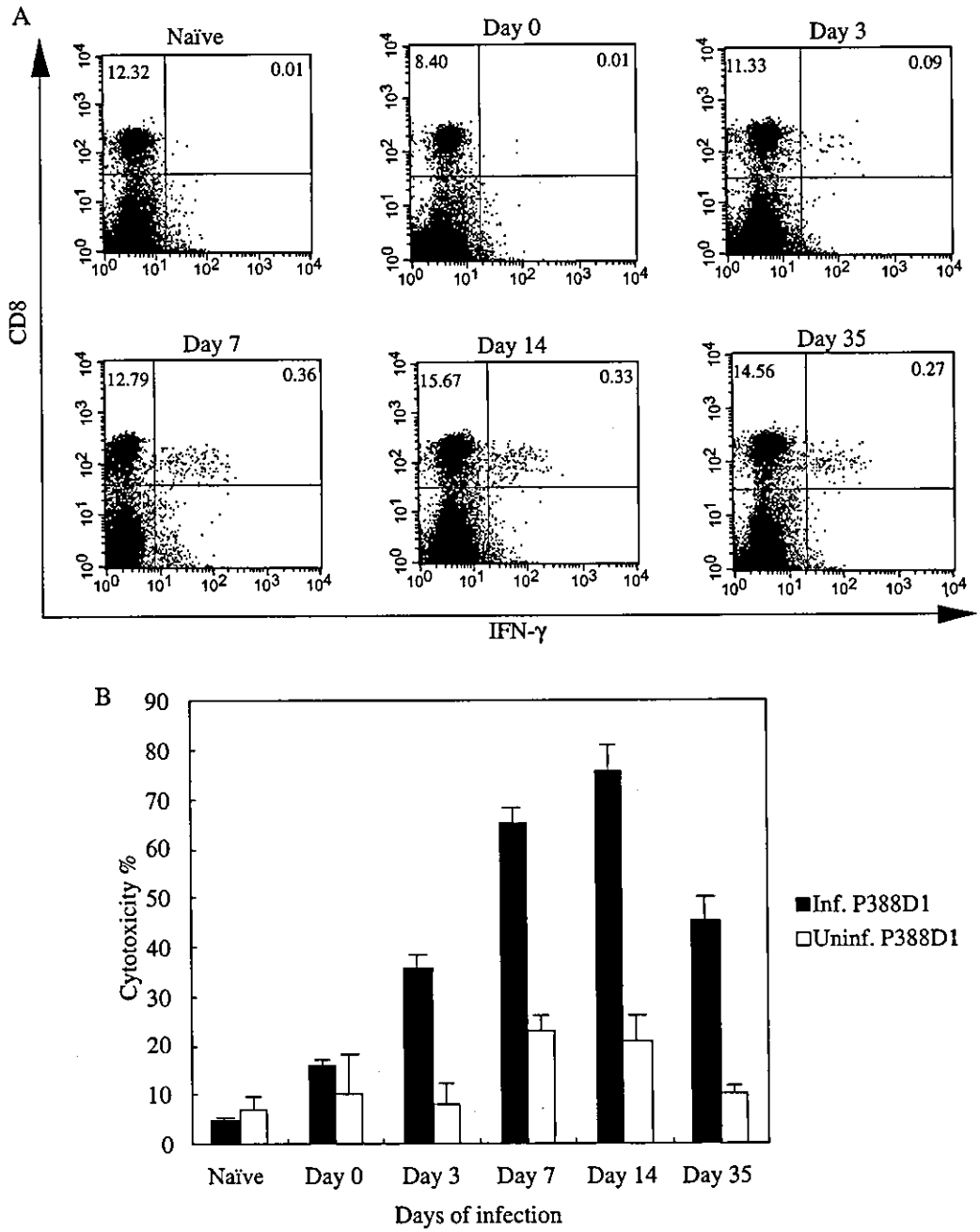

Fig. 3. Cytotoxic activity of spleen cells obtained from HTNV-infected mice. **A** Representative data for IFN-γ -producing HTNV-specific $CD8^+$ T cells from mice in Fig. 1 and uninfected mice. The gates were set for spleen cells. **B** Spleen cells from each mouse (presented in **A**) were used for the cytotoxicity assay. Spleen cells were cultured as described in Materials and methods. The spleen cells were tested using an LDH-release cytotoxicity assay. HTNV-infected P388D1 cells (Inf. P388D1) and uninfected P388D1 cells (Uninf. P388D1; negative control) were used as target cells. Bars represent the standard deviation. E/T ratio, 20

HTNV at 7, 14, and 35 days of age, no N protein was detected in the lungs (data not shown). These results demonstrate that there is a correlation between a lack of HTNV-specific CD8$^+$ T cells and the persistence of HTNV.

Cytotoxic activity and TNF-α production of HTNV-specific CD8$^+$ T cells

In the experiment described above, we measured IFN-γ in CD8$^+$ T cells stimulated with antigen-presenting cells to detect HTNV-specific CD8$^+$ T cells. Then, to analyze other functions of the HTNV-specific CD8$^+$ T cells, we examined cytotoxic activity and TNF-α production. Cytotoxicity of spleen cells, which included IFN-γ-producing CD8$^+$ T cells, was observed in mice inoculated with HTNV on days 3, 7, 14, and 35 after birth (Fig. 3). In contrast, in mice inoculated with HTNV on day 0, which had no IFN-γ-producing HTNV-specific CD8$^+$ T cells, no significant cytotoxicity to HTNV-infected target cells, as compared to uninfected target cells, was observed (Fig. 3). Levels of TNF-α production by IFN-γ-producing CD8$^+$ T cells were comparable among groups of mice inoculated with HTNV at 3, 7, 14, and 35 days of age (Fig. 4). Thus, IFN-γ-producing HTNV-specific CD8$^+$ T cells in immature mice inoculated with HTNV on days 3, 7, and 14 after birth were functionally similar to those of adult mice inoculated with HTNV on day 35 after birth with respect to TNF-α production and cytotoxic activity.

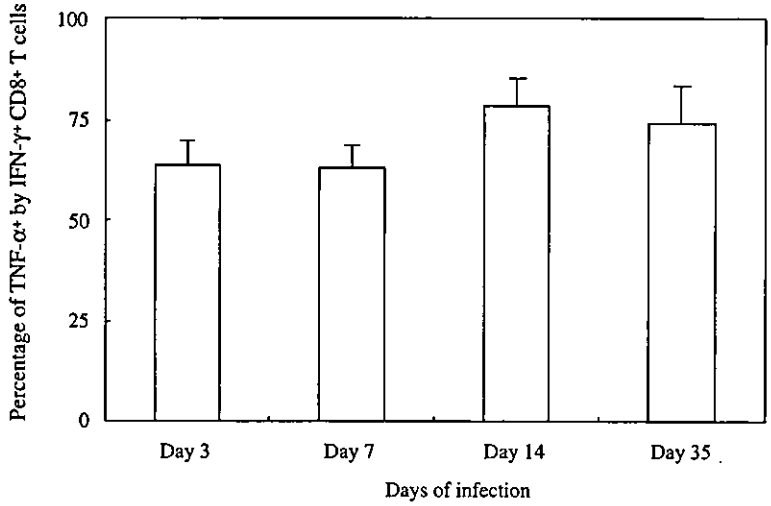

Fig. 4. TNF-α production by IFN-γ-producing CD8$^+$ T cells. TNF-α production was measured by using spleen cells that included the IFN-γ-producing HTNV-specific CD8$^+$ T cells, as shown in Fig. 1. To detect TNF-α$^+$ IFN-γ$^+$ CD8$^+$ T cells, spleen cells and HTNV-infected P388D1 cells were co-cultured at a ratio of 1:0.5 for 6 h in the presence of brefeldin A and IL-2. TNF-α production by IFN-γ$^+$ CD8$^+$ cells was detected using flow cytometry. Data represent the average percent of IFN-γ$^+$ CD8$^+$ T cells able to produce TNF-α. Bars represent the standard deviation

Discussion

In this study, to investigate differences in HTNV-specific $CD8^+$ T-cell responses between adult mice and newborn mice, we inoculated mice with HTNV on days 0, 3, 7, 14, and 35 after birth. The resulting HTNV-specific $CD8^+$ T-cell responses of mice inoculated on days 7 and 14 were similar to those of adult mice inoculated on day 35. On the other hand, the number of HTNV-specific $CD8^+$ T cells in mice inoculated with HTNV on day 3 was small compared to that of mice inoculated on days 7, 14, and 35 after birth. However, TNF-α production and the cytotoxic activity of IFN-γ-producing HTNV-specific $CD8^+$ T cells were not impaired in mice inoculated at 3 days of age. Generally, functional $CD8^+$ T cells are able to produce both IFN-γ and TNF-α, when stimulated with antigen-presenting cells, and to lyse target cells [5]. Wherry et al. proposed a model of functional exhaustion of $CD8^+$ T cells, in which partially function-exhausted $CD8^+$ T cells are unable to produce TNF-α or to lyse target cells, although they have the ability to produce IFN-γ [15]. Our findings suggest that individual HTNV-specific $CD8^+$ T cells induced in mice inoculated on day 3 after birth are functional, although the number of HTNV-specific $CD8^+$ T cells is small.

Previous studies have shown that HTNV causes symptomatic infection in newborn mice infected with high doses of HTNV [3, 6, 7, 14, 17]. However, in the present study, mice inoculated with 0.1 $NMLD_{50}$ of HTNV on days 0, 3, 7, 14, and 35 after birth developed asymptomatic infection (data not shown). In addition, persistent HTNV infection was observed in mice infected with HTNV within 24 h of birth (Day 0). It is known that natural rodent reservoirs of hantaviruses are persistently infected without signs of disease [8]. Therefore, it seems that the persistently HTNV-infected mice produced in this study could be useful as a model of persistent hantavirus infection.

In a previous study [2], we showed that HTNV persistence correlated closely with a lack of HTNV-specific $CD8^+$ T cells. Similar results were obtained in the present study (Fig. 2). These data strongly suggest that HTNV-specific $CD8^+$ T cells interrupt persistence of HTNV in mice. In natural rodent reservoirs, persistent hantavirus infection might be established by a lack of hantavirus-specific $CD8^+$ T cells, as observed in this model of persistent HTNV infection in mice.

In conclusion, the current findings show that mice over the age of 7 days have the ability to induce functional HTNV-specific $CD8^+$ T-cell responses that are indistinguishable from adult mice. However, it remains unclear why the number of HTNV-specific $CD8^+$ T cells induced in mice inoculated with HTNV on day 3 after birth is small. Further study will be necessary to resolve this question.

Acknowledgments

K. A. is a research fellow of the Japan Society for the Promotion of Science (JSPS) and was supported by a JSPS Research Fellowship for Young Scientists. This work was supported, in part, by Grants-in-Aid for Scientific Research and the Development of

Scientific Research from the Ministry of Education, Culture, Sports, Science and Technology, Japan.

Textcheck (English consultants) revised the English in the final draft of the manuscript.

References

1. Araki K, Yoshimatsu K, Ogino M, Ebihara H, Lundkvist A, Kariwa H, Takashima I, Arikawa J (2001) Truncated hantavirus nucleocapsid proteins for serotyping hantaan, seoul, and dobrava hantavirus infections. J Clin Microbiol 39: 2397–2404
2. Araki K, Yoshimatsu K, Lee BH, Kariwa H, Takashima I, Arikawa J (2003) Hantavirus-specific CD8(+)-T-cell responses in newborn mice persistently infected with Hantaan virus. J Virol 77: 8408–8417
3. Ebihara H, Yoshimatsu K, Ogino M, Araki K, Ami Y, Kariwa H, Takashima I, Li D, Arikawa J (2000) Pathogenicity of Hantaan virus in newborn mice: genetic reassortant study demonstrating that a single amino acid change in glycoprotein G1 is related to virulence. J Virol 74: 9245–9255
4. Elliott RM, Bouloy M, Calisher CH, Goldbach R, Moyer JT, Nichol ST, Pettersson R, Plyusnin A, Schmaljohn CS (2000) Family *Bunyaviridae*. In: van Regenmortel MHV, Fauquet CM, Bishop DHL, Carstens EB, Estes MK, Lemon SM, Maniloff J, Mayo MA, McGeoch DJ, Pringle CR, Wickner RB (eds) Virus taxonomy: classification and nomenclature of viruses. Seventh report of the International Committee on Taxonomy of Viruses. Academic Press, San Diego, CA, pp 599–621
5. Harty JT, Tvinnereim AR, White DW (2000) CD8$^+$ T cell effector mechanisms in resistance to infection. Annu Rev Immunol 18: 275–308
6. Kim GR, McKee KT Jr (1985) Pathogenesis of Hantaan virus infection in suckling mice: clinical, virologic, and serologic observations. Am J Trop Med Hyg 34: 388–395
7. McKee KT Jr, Kim GR, Green DE, Peters CJ (1985) Hantaan virus infection in suckling mice: virologic and pathologic correlates. J Med Virol 17: 107–117
8. Meyer BJ, Schmaljohn CS (2000) Persistent hantavirus infections: characteristics and mechanisms. Trends Microbiol 8: 61–67
9. Park JM, Cho SY, Hwang YK, Um SH, Kim WJ, Cheong HS, Byun SM (2000) Identification of H-2K(b)-restricted T-cell epitopes within the nucleocapsid protein of Hantaan virus and establishment of cytotoxic T-cell clones. J Med Virol 60: 189–199
10. Schmaljohn C, Hjelle B (1997) Hantaviruses – a Global Disease Problem. Emerg Infect Dis 3: 95–104
11. Schmaljohn CS, Jennings GB, Hay J, Dalrymple JM (1986) Coding strategy of the S genome segment of Hantaan virus. Virology 155: 633–643
12. Schmaljohn CS, Schmaljohn AL, Dalrymple JM (1987) Hantaan virus M RNA: coding strategy, nucleotide sequence, and gene order. Virology 157: 31–39
13. Schmaljohn CS (1990) Nucleotide sequence of the L genome segment of Hantaan virus. Nucleic Acids Res 18: 6728
14. Tamura M, Asada H, Kondo K, Tanishita O, Kurata T, Yamanishi K (1989) Pathogenesis of Hantaan virus in mice. J Gen Virol 70: 2897–2906
15. Wherry EJ, Blattman JN, Murali-Krishna K, Van Der Most R, Ahmed R (2003) Viral persistence alters CD8 T-cell immunodominance and tissue distribution and results in distinct stages of functional impairment. J Virol 77: 4911–4927
16. White JD, Shirey FG, French GR, Huggins JW, Brand OM, Lee HW (1982) Hantaan virus, aetiological agent of Korean haemorrhagic fever, has Bunyaviridae-like morphology. Lancet 1: 768–771

17. Yoo YC, Yoshimatsu K, Yoshida R, Tamura M, Azuma I, Arikawa J (1993) Comparison of virulence between Seoul virus strain SR-11 and Hantaan virus strain 76-118 of hantaviruses in newborn mice. Microbiol Immunol 37: 557–562
18. Yoshimatsu K, Arikawa J, Yoshida R, Li H, Yoo YC, Kariwa H, Hashimoto N, Kakinuma M, Nobunaga T, Azuma I (1995) Production of recombinant hantavirus nucleocapsid protein expressed in silkworm larvae and its use as a diagnostic antigen in detecting antibodies in serum from infected rats. Lab Anim Sci 45: 641–646

Author's address: Jiro Arikawa, Institute for Animal Experimentation, Graduate School of Medicine, Hokkaido University, Kita-15, Nishi-7, Sapporo 060-8638, Japan; e-mail: j_arika@med.hokudai.ac.jp